Widely Tunable Grating Cavity Lasers

Oh-Kee Kwon, Eundeok Sim, Kang-Ho Kim, Jong-Hoi Kim, Ho-Gyeong Yun, O Kyun Kwon, and Kwang Ryong Oh

A widely tunable multi-channel grating cavity laser is proposed and experimentally demonstrated. The device is implemented in Littman configuration with an echelle grating based on Rowland circle construction and realized by monolithically integrating all elements in an InP substrate. Lasing wavelength is selected by turning on an amplifier and the appropriate channel element in the array, and it is tuned by controlling light deflection electrically. The 6-channel device exhibits a tuning range of about 50 nm with a side mode suppression ratio of more than 30 dB. This is accomplished by adjusting the applied current of the dispersive element and phase control section.

Keywords: Tunable lasers, multi-channel lasers, grating cavity lasers, beam deflection, monolithic integration.

I. Introduction

Wavelength tunable lasers are needed for a wide variety of wavelength division multiplexing (WDM) packet switching architectures (PSA), and reconfigurable optical add/drop multiplexing (ROADM) networks, since they effectively employ wavelength resources, reduce inventory costs, and simplify network control software. Moreover, numerous applications in biophysics and environmental engineering become feasible with the availability of these light sources.

A number of tunable laser solutions have been proposed, which can be classified into four different categories. The simplest tunable laser is a distributed feedback (DFB) laser in which heat-sink temperature is used to tune the emission wavelength. With this approach, the tuning range is limited to 13 nm, and since the DFB laser operates at a high temperature, the output power is limited. Recently, multi-channel DFB arrays with a multimode interference (MMI) coupler and a semiconductor optical amplifier (SOA) [1] or with an external micro-electromechanical (MEM) mirror [2] showing a wide tuning range and high output power have been reported; but these configurations must deal with the requirement of having a number of closely spaced DFBs all working to tight specifications. A second approach uses a distributed Bragg reflector (DBR) laser. The emission wavelength can be tuned by injecting current into the DBR regions [3]. Recently a multi-channel DBR array with an MMI optical coupler and an SOA has been reported showing a wide tuning range and high output power [4]. Advanced designs of DBR lasers such as a sampled grating DBR laser [5], and a grating-assisted co-directional coupler with a rear sampled reflector (GCSR) laser [6] have been proposed, showing that a wide tuning range can be obtained. However, their recent structures have at least four electrodes which require complex multi-sectional current

Manuscript received Mar. 15, 2006; revised June 05, 2006.

Oh-Kee Kwon (phone: + 86 42 860 1366, email: okkwon@etri.re.kr), Eundeok Sim (email: sed63252@etri.re.kr), Jong-Hoi Kim (email: jonghoi@etri.re.kr), Ho-Gyeong Yun (email: yunhg@etri.re.kr), O Kyun Kwon (email: okyun@etri.re.kr), and Kwang Ryong Oh (email: kroh@etri.re.kr) are with IT Convergence & Components Laboratory, ETRI, Daejeon, Korea.

Kang-Ho Kim (email: khkim01@kopti.re.kr) is with Department of LED/SSL R&DB Sector, Korea Photonics Technology Institute, Gwangju, Korea.

control algorithms [7], [8] and require a very low facet reflection [9]. MEM-tunable vertical-cavity surface-emitting lasers (VCSELs) are the product of a third approach to realizing tunable lasers. It is usually difficult to realize high power VCSELs at the operating wavelength of 1.55 μm by electric pumping. Instead, high power can be obtained by optical pumping alone [10]. This configuration needs an additional pumping laser and has a lower energetical efficiency. The last approach uses external-cavity diode laser technology. This technology is widely used to provide tunable lasers for test and measurement applications. Wide tuning ranges with high output powers and good spectral properties have been demonstrated by external-cavity tunable lasers (ECTLs). Wavelength tuning can be achieved by the rotation and/or translation of one element of the cavity [11]-[13]. However, because ECTLs include moving parts, the long-term reliability of this technology for components might be a problem. Moreover, due to its mechanical tuning it is difficult to achieve high-speed tuning. To provide stable operation (against vibration) and a fast tuning rate, electrically tunable external cavity lasers have been proposed [14]-[17]. Most of them, however, are large and/or low in optical power because of their size and the high insertion loss of tuning elements, while extremely wide tuning ranges with high powers and high SMSRs has been demonstrated in [17].

In addition to tunable laser solutions, methods generating multi-wavelength output from a single laser chip with wavelength control have been proposed [18]-[27]. These methods have been developed as low cost WDM sources because of their simple implementation, good wavelength accuracy, and good integration compatibility. One method uses an arrayed waveguide grating (AWG)-based laser which has an array of SOAs on one side of an AWG. Wavelength selectivity is provided by the AWG, and the lasing wavelength is selected by turning on the appropriate element in the SOA array. Simultaneous emission of 11 wavelengths that are spaced 3.2 nm apart was achieved [20]. More sophisticated designs of multi-wavelength lasers, which are called digitally tunable lasers, have been proposed, generating more wavelengths with fewer channels and improving single-mode stability and output power [21]-[23]. However, their operational conditions are rather complex and strongly affected by facet reflections. Another method uses a grating cavity laser in which a diffraction grating provides wavelength selectivity [24]. Soole and others reported a wavelength-selectable laser integrated with an SOA array and a Rowland circle grating. Lasing was obtained at 15 discrete wavelengths with a channel spacing of 1.89 nm from 1507 to 1535 nm [25]. Asghari and others reported an integrated multichannel grating cavity laser based on the integration of an SOA array with a transmission grating and two focusing mirrors. Two wavelengths with a channel spacing of 21 nm were obtained [26].

Recently, we proposed and demonstrated a novel tunable laser based on the grating cavity configuration [27]. This device was realized by monolithically integrating a semiconductor optical amplifier (SOA), a phase-control section (PCS), a dispersive element (DE), and an etched diffraction grating (EDG) into a single chip. Wavelength tuning was also achieved by injecting current only into the DE and PCS. This laser is expected to have high long-term reliability and a rapid tuning rate owing to its monolithic integration and electrical tuning, respectively. Moreover, good operational and spectral properties were obtained, although its facets (cleaved facet and grating facet) were uncoated.

Still, it was difficult to obtain a wide tuning range and high SMSR at the same time because of the limited deflection angle variation of the dispersive pattern resulting from a relatively small amount of modal change in the refractive index. In order to overcome this problem, the use of guide-core material with lower band-gap energy can extend the tuning range, but absorption will be drastically increased [28]. Instead, by combining a multi-channel structure [29], we propose a new type of tunable multi-channel grating cavity laser with an extended tuning range.

The paper is organized as follows: In section II, the design and operating principles of the proposed device are described. In section III the fabrication of the device is described in detail. In Section IV, the experimental results are shown and reported. Section V concludes the paper.

II. Design and Operating Principles

A schematic diagram showing the monolithically integrated tunable N-channel grating cavity laser is depicted in Fig. 1. The device was implemented in Littman configuration with an echelle grating based on Rowland circle construction. Lasing wavelength can be selected by turning on an SOA and the appropriate channel element in the array since different channels lase at different wavelengths in accord with their diffraction angle β_i for the incident angle of the beam at the grating pole α.

Output power can be obtained through one port without an optical combiner. The grating was aberration-free up to the fifth order by tailoring its period (d_0 = 4.4 μm) at the pole, and each grating facet was individually blazed, where the blazed angle is $(\alpha + \beta_{N/2})/2$. The channel separations between the two waveguides on the Rowland circle were designed by the proper selection of the channel spacing $\Delta\lambda_{CH}$ for given grating radius R and diffraction order m. The channel outputs were separated

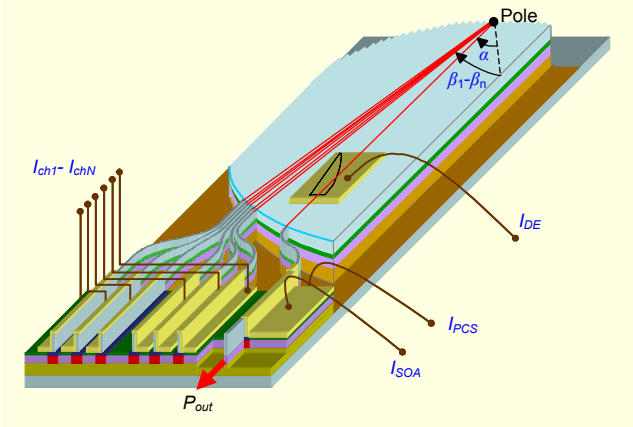

Fig. 1. A schematic diagram of the proposed laser. I_{SOA}, I_{PCS}, I_{DE}, and I_{ch1}-I_{chN} are the SOA, PCS, DE, and channel currents, respectively.

by gaps of about 150 μm in order to avoid an unwanted selective area growing between channels.

Wavelength tuning $\Delta\lambda$ of each channel is based on electrically controlled beam deflection provided by the pattern of the dispersive element. This beam deflection changes the incident angle of the beam on the grating $\Delta\alpha$ and, thus, tunes the diffraction wavelength from the grating according to the Littman condition.

Figure 2 shows a schematic view of the dispersive pattern. This pattern has two interfaces along the optical path of the beam and one side of the pattern area is designed perpendicular to the straight waveguide (point O). To determine the curve of the other boundary, we consider the light that is focused to point Q after diffraction by the grating. Here, the phase difference between two adjacent grating elements must be equal to a multiple of 2π for the lasing wavelength λ. The N-th phase difference $\Delta\Phi_N$ between the light reflected by the grating facets centered at P_N (N-th element) and P_0 (pole) points can be expressed by

$$\begin{aligned}\Delta\Phi_N &= \Phi_{\overline{OP_N}} - \Phi_{\overline{OP_0}} \\ &= \frac{2\pi}{\lambda}\left[n_0\left(L_{N1}+L_{N2}\right)-\left(n_0-n_D\right)l_N\right] \\ &\quad -\frac{2\pi}{\lambda}\left[n_0\left(L_{01}+L_{02}\right)-\left(n_0-n_D\right)l_0\right]=2\pi mN, \end{aligned} \quad (1)$$

where n_D and n_0 are the effective refractive index of the inside and outside of the dispersive pattern, respectively.

By injecting the current into the dispersive pattern, the material refractive index of guide-core n_{core} is directly changed and, thus, n_D can be written as $n_D = \Gamma n_{core} + (1-\Gamma)n_{clad}$ (where Γ is the optical confinement factor and n_{clad} is the material refractive index of the cladding layer). If we assume

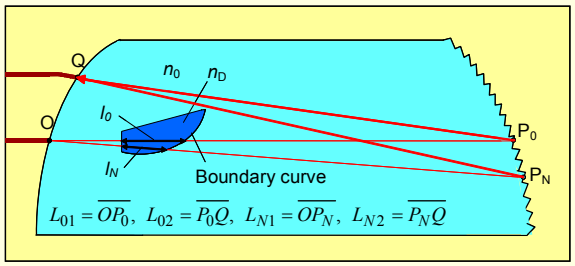

Fig. 2. A schematic view of the dispersive pattern.

that the path length variation after the beam deflection is small, then the wavelength tuning $\Delta\lambda$ can be expressed by

$$\Delta\lambda = -\frac{\Gamma\Delta n_{core}}{mN}\left(l_0 - l_N\right), \quad (2)$$

where Δn_{core} is the material refractive index of change of the guide-core within the dispersive pattern. Compared to our past work [27], the tuning range is half for the same incident angle because the angular dispersion of the Littman configuration is twice as large as that of Littrow. A boundary curve can be obtained from the traces of l_N with an increase of N for given m, l_0, and $\Delta\lambda/\Gamma\Delta n_D$. We note that Δn_{core} is decreased with the increase of the current due to the carrier-induced change in the refractive index and, thus, $\Delta\lambda$ becomes positive for $l_0 > l_N$ and negative for $l_0 < l_N$. With consideration of past experimental results, the dispersive pattern was designed for tuning to the longer wavelength side (l_0=350 μm and $\Delta\lambda/\Gamma\Delta n_D$ = 7 nm/(-0.01) for the device with R = 3 mm and m = 5).

III. Fabrication

The epitaxial layers were grown by low pressure metal-organic chemical vapor deposition (LP-MOCVD). The fabricated devices were based on ridge waveguide structures in InP-based materials. In monolithic integration between active and passive waveguides, we used a butt-joint coupling method [30] which has great advantages of not only completely separate optimization of each section in terms of thickness, composition, and electrical properties, but also convenience and flexibility of design.

Figure 3 shows the processing steps for the fabrication of the tunable lasers. The starting point of the processing as described here is the layer stack of the active section (first grown epitaxial layers). This layer stack consists of an n-InP substrate, an n-InP lower cladding layer, an active region, a p-InP first upper cladding (doping $d = 5\times10^{17}$cm^{-3}, thickness t = 0.1 μm), a p-InGaAsP etch-stop layer (bandgap wavelength λ_{bg}=1.24 μm,

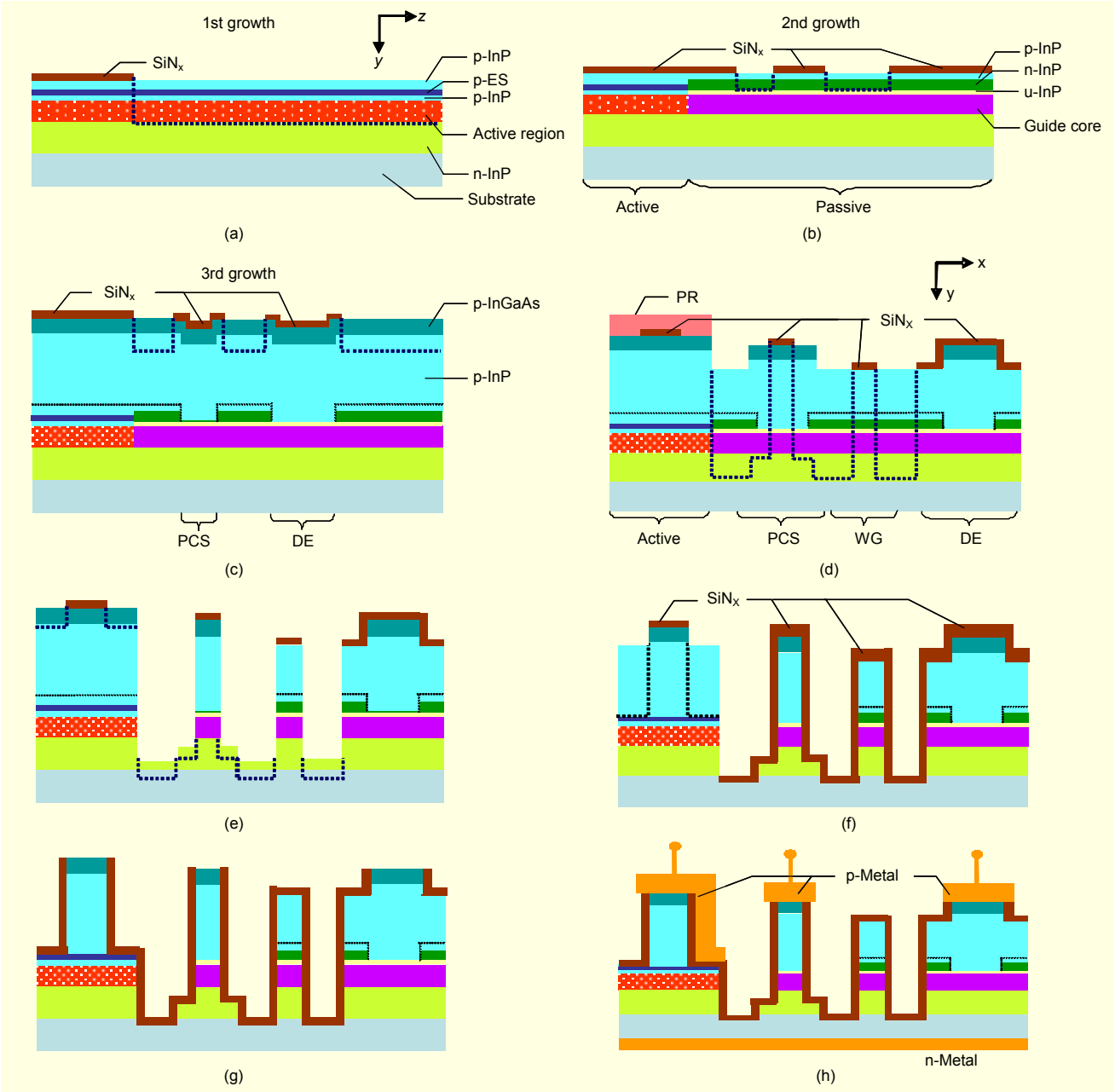

Fig. 3. Processing steps for the fabrication of tunable lasers. (a)-(c) are the side section area of the device and (d)-(h) are the cross section area. x-, y-, z-axes are lateral, vertical, and longitudinal direction, respectively.

t = 0.01 μm), and a p-InP second upper cladding layer (t = 0.3 μm). The active region contains a multiple quantum well (MQW) and a two-step separate confinement hetero-structure (TS-SCH) layer. The MQW is composed of seven 7-nm-thick InGaAsP wells (λ_{bg}=1.68 μm, compressive 0.8%) and eight 10-nm-thick barriers (λ_{bg}=1.3 μm, tensile 0.6%). The TS-SCH layer consists of a 50 nm-thick inner layer (λ_{bg}=1.24 μm) and a 50 nm-thick outer layer (λ_{bg}=1.08 μm). After defining SiN_x-masks with a width of 20 μm (image pattern of an SOA and channels), the active layer stack was etched using dry etching (CH_4/H_2 reactive-ion etching (RIE)) and wet chemical etchings (H_2SO_4, $HBr:H_2O_2:H_2O$ = 8:2:100, and Semico-clean) as shown in Fig. 3(a). The second grown layer stack consists of a guide-core (λ_{bg}=1.24 μm, t = 0.35 μm), an undoped-InP layer (t = 0.1 μm), an n-InP ($d = 5\times10^{17}cm^{-3}$, t = 0.25 μm) an upper cladding layer, and a p-InP layer ($d = 5\times10^{17}cm^{-3}$, t = 0.05 μm). We note here that the n-InP works as a current blocking layer. After defining the SiN_x masks (image-reversal pattern of PCS and DE), trenches were formed so that the injected currents would flow only within the PCS and DE sections as in Fig. 3(b).

After removal of the SiN_x masks, the third grown layers were stacked and then dry etching was done for electrical isolations (Fig. 3(c)). For the fabrication of the grating and the deep ridge waveguides simultaneously, the active section, PCS, waveguides, DE, and the grating were patterned by using SiN_x and photo-resist (PR) as etching masks (Fig. 3 (d)). The dry-etching (CH_4:H_2 = 6.2:21, Etched rate = 0.35 μm/min, verticality < 3°) was done to a depth of approximately 3 μm and micro-ashing and H_2SO_4 were added to remove residual polymers attached to the deeply etched walls. After the removal of the PR mask from the active section, additional dry-etching was performed as in Fig. 3(e). After the opening of the active section with the SiN_x mask, the shallow ridge shape of the active section was formed to the etch-stop layer using selective InP wet etching (HCl:H_3PO_4 = 15:85) (Fig. 3(f)). A contact opening in the SiN_x etching mask was performed (Fig. 3(g)) and then metalizations were done (Fig. 3(h)). The metalization layer stack was evaporated on the top (Ti/Pt/Au=30/50/300 nm) and back (Cr/Au=50/250 nm) of the wafer.

Figure 4 shows an image of the chip after scribing. The SOA and channels had shallow-ridge waveguides, the width of which was 2.8 μm. The guide sections each had a deep-ridge and their widths were designed for maximizing mode coupling between shallow- and deep-ridges (4.5 μm), to achieve higher spectral resolution of the grating (2.5 μm), and to improve the mode-coupling with a lensed fiber (2.5 μm). The results related to this were described in more detail in [29].

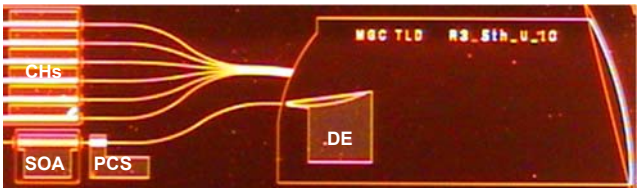

Fig. 4. The chip picture of the fabricated device (R = 5 mm and m = 5). SOA, PCS, and channel lengths are 500, 150, and 650 μm, respectively. Chip size is 1.5×5.5 mm^2.

IV. Experimental Results

1. Mode Stability

The etched concave grating in this device is used as an intra-cavity wavelength filter that sets the operating wavelengths provided by an amplifier and channels. The grating spatially separates the different wavelengths along the Rowland circle so that they can be individually controlled by current injection into the appropriate channel while all of the wavelengths are available in a single output waveguide. The filter passband width (grating resolution) is determined by the diffraction order m and the number of the illuminated part of the grating which depends on the grating period d, grating radius R, and the waveguide widths on the Rowland circle. The full width half maximum (FWHM) of about 2 nm was typically obtained for the structure with m equal to 5 and R equal to 3 mm. Since the mode spacing corresponding to the total cavity length (approx. 0.03 nm ; $\lambda^2/2n_gL$, where λ=1.55 μm, n_g=3.7, and L=2×5.5 mm) is much narrower than the grating resolution, many longitudinal modes exist within the passband width. This corresponds to the intermediate filter case in [31]. Various nonlinear phenomena such as mode-jumps with the operating current, bi-stability in frequency, and hysteresis in the L-I curve were also observed in this device. As for (dynamic) mode stability, one of the most important features in long-cavity lasers, it was reported that a single longitudinal mode operation with an SMSR in a range lower than from 10 to 30 dB could be guaranteed theoretically [32]-[34]. We also found experimentally that an SMSR of more than 30 dB could be obtained even without adjusting the PCS current [27], [29], [35]. The reason for this is mainly that the beating of the main mode with the side modes causes a spatial modulation in the carrier densities of the active region (namely, interband gain nonlinearity), and, as a result, the longitudinal modes of the longer wavelength side experience a higher gain and those of the shorter side are suppressed [36], [37]. This can lead to single-mode stability. In this structure, the linewidth and/or SMSR of the lasing mode can be further improved by slightly controlling the PCS current.

Figure 5 shows the typical power spectra of the fabricated devices, as measured from the output of an SOA using a tapered fiber under the CW operation (22°C). The 6-channel laser ($\Delta\lambda_{CH}$ = 5.5 nm, R = 3 mm, and m = 6) was operated at an SOA current of 120 mA, with channel currents in a range from 100 to 140 mA, and a PCS current of approximately 10 mA. Here, the channel currents were adjusted to obtain the fiber coupled peak power of about 0dBm and the PCS current was controlled to get the maximum SMSR. The 8-channel lasers ($\Delta\lambda_{CH}$ = 4.5 nm, R = 4.2 mm, and m = 6) were also operated at an SOA current of 120 mA with channel currents in a range from 120 to 150 mA (fiber coupled peak power of about -5 dBm). The amplified spontaneous emission (ASE) noises of both devices were greatly reduced and good SMSRs (about 45 dB for (a) and 40 dB for (b)) were obtained over all channels. However, the ripples of ASE still remained with the period of about 0.5 nm which corresponds to the length of 650 μm (from the output facet to the right boundary of the SOA and/or channel length). Their peak-to-peak values were about 2dB for (a) and 1.7 dB for (b), and these also increased with the SOA current. As the grating radius R increased, the mode stability on lasing modes improved (namely, the pedestal width of the lasing modes became narrower and the wavelength

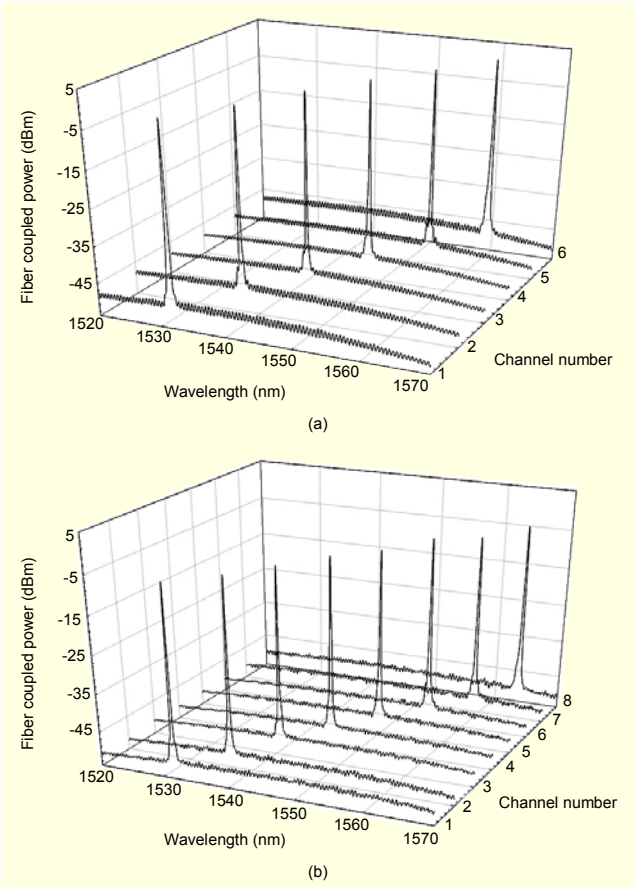

Fig. 5. Superimposed power spectra of (a) 6-channel laser ($\Delta\lambda_{CH}$ = 5.5 nm, R = 3 mm, and m = 6) and (b) 8-channel laser ($\Delta\lambda_{CH}$ = 4.5 nm, R = 4.2 mm, and m = 6). The resolution of optical spectrum analyzer was 0.1 nm.

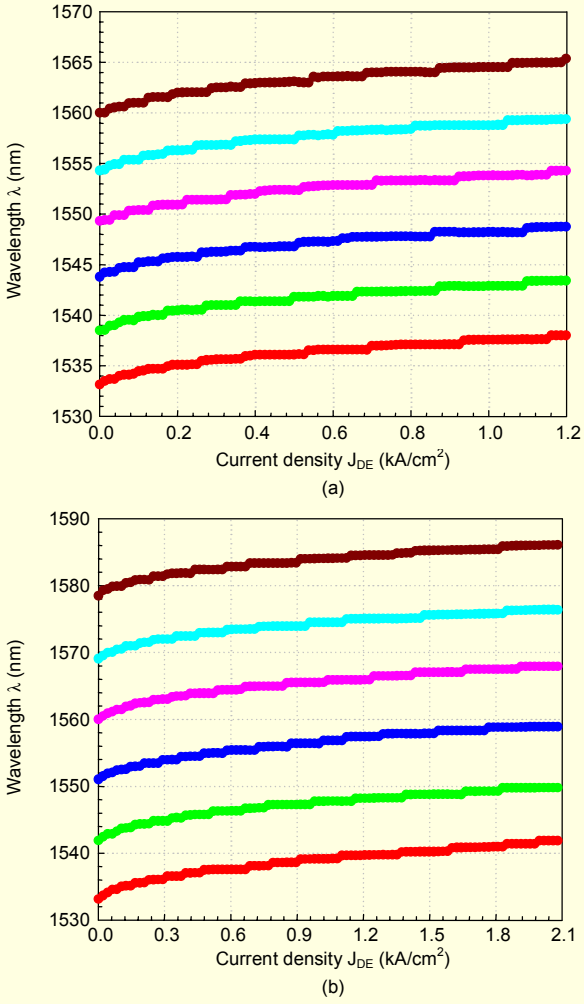

Fig. 6. Tuning curves of 6-channel lasers (R = 3 mm and m = 5) with (a) $\Delta\lambda_{CH}$ = 5.5 nm and (b) $\Delta\lambda_{CH}$ = 8.5 nm. J_{DE} (= I_{DE}/Area of dispersive pattern (about 2.4×10^4 μm^2)) is the current density of dispersive element.

variation with change in operating currents was reduced). We attribute this to the narrowness of the grating resolution which results from increasing the area illuminated on the grating. On the contrary, the output powers and SMSRs are decreased. These are consequences of the reduction of the feedback intensity which results from the increase in passive loss.

2. Wavelength Tuning

Figure 6 shows the tuning curves of two 6-channel Littman-type grating cavity lasers (R = 3 mm and m = 5). They both have the same structural parameters except the channel spacings, $\Delta\lambda_{CH}$ = 5.5 nm (a) and 8.5 nm (b). As expected, overall tuning ranges of 33 nm (6×5.5 nm, 1533 nm – 1566 nm) for (a) and 51 nm (6×8.5 nm, 1533 nm – 1584 nm) are shown. In this experiment, it was found that with the increase of the dispersive current, the pedestal of the lasing mode moved to the longer wavelength side continuously, but its peak wavelength moved did discretely (mode jumping, stair-like shape). The mode was jumped at the wavelength interval of about 0.5 nm and fluctuated between stable and unstable with the dispersive current. In addition to this result, we observed that at an SOA current of 40 mA (and a channel current of 120 mA) where the ASE ripple was considerably weak (< 0.1 dB) the wavelength of the lasing mode moved somewhat randomly with the relatively small wavelength interval (< 0.1 nm) by increasing the dispersive current. These experimental results can be summarized and analyzed as follows.

1) The internal reflection between the active and passive regions should act as another intra-cavity filter with the wavelength interval of 0.5 nm.
2) The dispersive current changes the phase of the light diffracted from the grating and also shifts the grating passband. This originates from our assumption about dispersive pattern design; namely, the path length difference due to the refraction

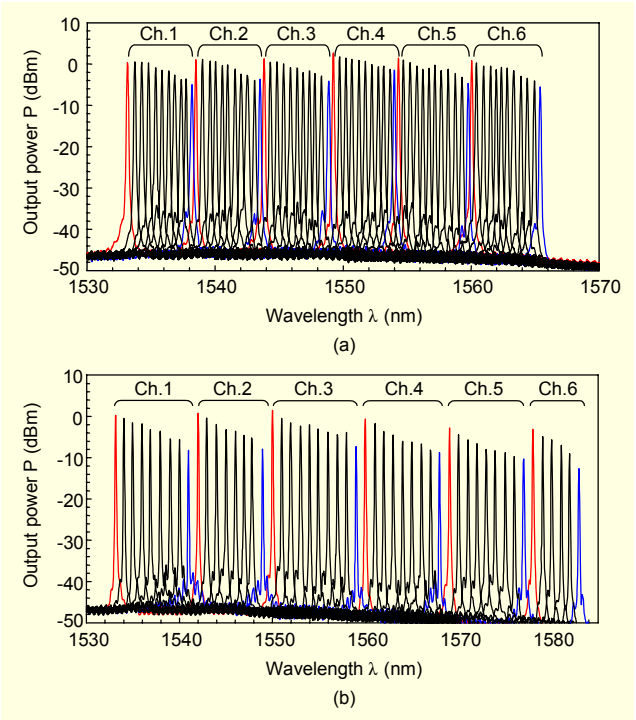

Fig. 7. Superimposed power spectra for (a) and (b) in Fig. 6. The spacing between wavelengths is about 0.5 nm for (a) and about 1 nm for (b).

of the light at each pattern boundary was neglected. Regarding this phase change effect we conclude that when the dispersive current is increased, the optical length is varied by the path length difference, hence its variation changes the phase of the diffracted light. This change induces the phase mismatch between the light emitted from the active region and the light diffracted from the grating. As a result, this effect can make the linewidth of the lasing mode broader or narrower. In practice, of course, it happens at the same time as the shift of the grating passband.

3) The wavelength tuning is also affected by intra- and inter-gain nonlinearities as shown in Fig. 3 of [27].

Fortunately, in this device this unwanted phase variation can be overcome by slightly controlling the PCS current; therefore, a stable mode can be obtained within the tuning range by the combination of the dispersive and PCS currents.

Figure 7 shows the superimposed output spectra for (a) and (b) in Fig. 6. In the case of (a), the spectra were obtained by slightly adjusting I_{PCS} under I_{SOA} =100 mA and I_{CHs} = 110~120 mA. In the case of (b), the SOA and channel currents were differently injected (100 mA (I_{SOA})/100 mA (I_{CH}) for channels 1 to 4, 150 mA/150 mA for channel 5, and 200 mA/200 mA for channel 6). Still, the output power of channels 5 and 6 is lower than that of channels 1 through 4. This is because the operating wavelengths of channels 5 and 6 deviate greatly from the gain peak (peak wavelength 1545 nm). Secondly, the diffraction conditions of the channels except channel 3 are deviated from the blaze angle. Therefore, to reduce the power difference among the channels, active materials with broad and flat gain [38] and waveguide structures with small waveguide separations may be required.

Both devices initially have high powers and good spectral properties. However, output power and SMSRs become deteriorated with the increase of dispersive current. This is mainly due to the reduction of the feedback intensity resulting from the increase of the optical losses within the dispersive patterns. The peak power differences over channel tuning ranges were from 0.9 to 1.1 dB/nm (= 5~6 dB/5.5 nm) for (a) and from 1 to 1.2 dB/nm (= 8.5~10.5 dB/8.5 nm) for (b). This problem can be overcome to some degree by the control of the SOA and/or channel currents during wavelength tuning. However, this method may make the tuning operation complex. Instead, a dispersive element using a coupled quantum well [39] could be one alternative. Ways to achieve additional improvements in the high fiber-coupled output power (> 10 dBm), low peak power difference (< 3 dB), and broad tuning range (that is, C+L band) are the subject of future investigations. Work towards realizing structures with improved performance is ongoing.

V. Conclusion

In conclusion, to achieving a wide tuning range and a high SMSR simultaneously, we proposed, fabricated, and demonstrated a monolithically integrated multi-channel grating cavity laser with a dispersive element. For a 6-channel device with a 3 mm-grating radius and a fifth diffraction order, a tuning range of about 50 nm and an SMSR of more than 30 dB were achieved. The tuning range can easily be extended by increasing the number of channels. This device has high reliability and a rapid tuning rate owing to its monolithic integration and electrical tuning, respectively. Moreover, it is expected to be a low cost tunable and/or multi-wavelength source because it can be easily fabricated using standard patterning or etching techniques and, besides, it does not need to be dielectric/metallic-coated on the cleaved /grating facet.

References

[1] H. Hatakeyama, K. Naniwae, K. Kudo, N. Suzuki, S. Sudo, S. Ae, Y. Muroya, K. Yashiki, K. Satoh, T. Morimoto, K. Mori, and T. Sasaki, "Wavelength-Selectable Microarray Light Sources for S-, C-, and L-B and WDM Systems," *IEEE Photon. Technol. Lett.*, vol. 15, no. 7, July 2003, pp. 903-905.

[2] B. Pezeshiki, E. Vail, J. Kubicky, G. Yoffe, S. Zou, J. Heanue, P. Epp, S. Rishton, D. Ton, B. Faraji, M. Emanuel, X. Hong, M.

Sherback, V. Agrawal, C. Chipman, and T. Razazan, "20-mW Widely Tunable Laser Module Using DFB Array and MEMS Selection," *IEEE Photon. Technol. Lett.*, vol. 14, no. 10, Oct. 2002, pp. 1457-1459.

[3] T.L. Koch, U.Koren, and B. I. Miller, "High Performance Tunable 1.5mm InGaAs/InGaAsP Multiple Quantum Well Distributed Bragg Reflector Lasers," *Appl. Phys. Lett.* vol. 53, Sep. 1988, no. 12, pp. 1036-1038.

[4] H. Arimoto, H. Sato, T. Kitatani, T. Tsuchiya, K. Shinoda, A. Takei, H. Uchiyama, M. Aoki, and S. Tsuji, "Wide-Wavelength-Range and High-Output-Power Short-Cavity DBR Laser Array with Active Distributed Bragg Reflector," *Proc. IEEE 19th Int'l Semiconductor Laser Conf.*, Matsue, Japan, Sept. 2004, pp. 141-142.

[5] V. Jayaraman, Z.M. Chuang, and L. A. Coldren, "Theory, Design, and Performance of Extended Tuning Range Semiconductor Lasers with Sampled Gratings," *IEEE J. Quantum Electron.*, vol. 29 , no. 6, June 1993, pp. 1824-1834.

[6] M. Öberg, S. Nilsson, K. Streubel, J. Wallin, L. Bäckborn, and T. Klinga, "74nm Wavelength Tuning Range of an InGaAsP/InP Vertical Grating Assisted Codirectional Coupler Laser with Rear Sampled Grating Reflector," *IEEE Photon. Technol. Lett.*, vol. 5 no. 7, July 1993, pp. 735-738.

[7] J. S. Barton, E. J. Skogen, M. L. Masanovic, S. P. Den Baars, and L.A. Coldren, "A Widely Tunable High-Speed Transmitter Using an Integrated SGDBR Laser-Semiconductor Optical Amplifier and Mach-Zehnder Modulator," *IEEE J. Select. Topics Quantum Electron.*, vol. 9, 2003, pp. 1113-1117.

[8] S. H. Oh, H. Ko, K. S. Kim, J. M. Lee, C. W. Lee, O. K. Kwon, S. Park, and M. H. Park, "Fabrication of Butt-Coupled SGDBR Laser Integrated with Semiconductor Optical Amplifier Having a Lateral Tapered Waveguide," *ETRI Journal*. vol. 27, no. 5, Oct. 2005, pp. 551-556.

[9] R. Todt and M. C. Amann, "Influence of Facet Reflections on Monolithic Widely Tunable Laser Diodes," *IEEE Photon. Technol. Lett.*, vol. 17, no. 12, Dec. 2005, pp. 2520-2522.

[10] D. A. Vakhshoori, J. H. Zhou, M. Jiang, M. Azimi, K. McCallion, C. C. Lu, K. J. Knopp, J. Cai, P. D. Wang, P. Tayebati, H. Zhu, and P. Chen, "C-Band Tunable 6mW Vertical-Cavity Surface-Emitting Lasers," *Proc. OFC 2000*, Paper PD13-1, 2000, pp. 205-207.

[11] J. D. Berger, D. Anthon, S. Dutta, F. Ilkov, and I. F. Wu, "Tunable MEMS Devices for Reconfigurable Optical Networks," *OFC 2005*, Anaheim, USA, paper OThD1, 2005.

[12] X. M. Zhang, A. Q. Liu, C. Lu, and D. Y. Tang, "Continuous Wavelength Tuning in Micromachined Littrow External-Cavity Lasers." *IEEE J. Quantum Electron*., vol. 41, no. 2, Feb. 2005, pp. 187-197.

[13] J. De Merlier, K. Mizutani, S. Sudo, K. Naniwae, Y. Furushima, S. Sato, K. Sato, and K. Kudo, "Full C-Band External Cavity Wavelength Tunable Laser Using a Liquid-Crystal-Based Tunable Mirror," *IEEE Photon. Technol. Lett.,* vol. 17, no. 3, Mar. 2005, pp. 681-683.

[14] G.A. Coquin and K.W. Cheung, "Electronically Tunable External-Cavity Semiconductor Laser," *IEE Electron. Lett*., vol. 24, no. 10, May 1988, pp. 599-600.

[15] M. Kourogi, K. Imai, B, Widyatmoko, T. Shimizu, and M. Ohtsu, "Continuous Tuning of an Electrically Tunable External-Cavity Semiconductor Laser," *Opt. Lett.*, vol. 25, no. 16, Aug. 2000, pp. 1165-1167.

[16] O. K. Kwon, K. H. Kim, E. D. Sim, H. K. Yun, J. H. Kim, H. S. Kim, and K. R. Oh, "Proposal of Electrically Tunable External-Cavity Laser Diode," *IEEE Photon. Tech. Lett.,* vol. 16, no. 8, Aug. 2004, pp. 1804-1806.

[17] K. Takabayashi, K. Takada, N. Hashimoto, M. Doi, S. Tomabechi, T. Nakazawa, and K. Morito, "Widely (132nm) Wavelength Tunable Laser Using a Semiconductor Optical Amplifier and an Acousto-Optic Tunable Filter," *IEE Electron. Lett*., vol. 40, no. 19, Sep. 2004, pp. 1187-1188.

[18] C. E. Zah, F. J. Favire, B. Pathak, R. Bhat, C. Caneau, P. S. D. Lin, A. S. Gozdz, N. C. Andreadakis, M. A. Koza, and T. P. Lee, "Monolithic Integration of Multiwavelength Compressive-Strained Multiquantum-Well Distributed-Feedback Laser Array with Star Coupler and Optical Amplifiers," *IEE Electron. Lett.*, vol. 28, no. 25, Dec. 1992, pp. 2361-2362.

[19] M. G. Young, U. Koren, B. I. Miller, M. A. Newkirk, M. Chien, M. Zirngibl, C. Dragone, B. Tell, H. M. Presby, and G. Raybon, "A 16×1 Wavelength Division Multiplexer with Integrated Distributed Bragg Reflector Lasers and Electroabsorption Modulators," *IEEE Photon. Technol. Lett*., vol. 5, no. 8, Aug. 1993, pp. 908-910.

[20] M. Zirngibl, B. Glance, L. W. Stulz, C. H. Joyner, G. Raybon, and I.P. Kaminow, "Characterization of a Multiwavelength Waveguide Grating Router Laser," *IEEE Photon. Technol. Lett.*, vol. 6, no. 9, Sep. 1994, pp. 1082-1084.

[21] C.R. Doerr, C.H. Joyner, and L.W. Stulz, "40-Wavelength Rapidly Digitally Tunable Laser," *IEEE Photon. Technol. Lett.*, vol. 11, no. 11, Nov. 1999, pp. 1348-1350.

[22] D. van Thourhout, L. Zhang, W. Yang, B. I. Miller, N. J. Sauer, and C. R. Doerr, "Compact Digitally Tunable Laser," *IEEE Photon. Technol. Lett.*, vol. 15, no. 2, Feb. 2003, pp. 182-184.

[23] J. H. den Besten, R. G. Broeke, M. van Geemert, J. J. M. Binsma, F. Heinrichsdorff, T. van Dongen, E. A. J. M. Bente, X. J. M. Leijtens, and M.K. Smith, "An Integrated 4×4-Channel Multiwavelength Laser on InP," *IEEE Photon. Technol. Lett.*, vol. 15, no. 3, Mar. 2003, pp. 368-370.

[24] P. A. Kirkby, "Multichannel Wavelength-Switched Transmitters and Receivers-New Component Concepts for Broad-Band Networks and Distributed Switching Systems," *J. Lightwave Tech.*, vol. 8, no. 2, Feb. 1990, pp. 202-211.

[25] J. B. D. Soole, K. R. Poguntke, A. Scherer, H. P. LeBlanc, C. Chang-Hasnain, J. R. Hayes, C. Caneau, R. Bhat, and M. A. Koza, "Wavelength-Selectable Laser Emission from a Multistripe Array Grating Integrated Cavity Laser," *Appl. Phys. Lett.*, vol. 61, no. 23, Dec. 1992, pp. 2750-2752.

[26] M. Asghari, B. Zhu, I. H. White, C. P. Seltzer, C. Nice, I. D. Henning, A.L. Burness, and G.H.B, Thompson, "Demonstration of an Integrated Multichannel Grating Cavity Laser for WDM Applications," *IEE Electron. Lett.*, vol. 30, no. 20, Sep. 1994, pp. 1674-1675.

[27] O. K. Kwon, J. H. Kim, K. H. Kim, E. D. Sim, H. S. Kim, and K. R. Oh, "Monolithically Integrated Grating Cavity Tunable Lasers," *IEEE Photon. Tech. Lett.,* vol. 17, Sep. 2005, pp. 1794-1796.

[28] B. R. Bennett, R. A. Soref, and Jesus A. Del Alamo, "Carrier-Induced Change in Refractive Index of InP, GaAs, and InGaAsP," *IEEE J. Quantum Electron.*, vol. 26, no. 1, Jan. 1990, pp. 113-122.

[29] O. K. Kwon, K. H. Kim, E. D. Sim, J. H. Kim, and K. R. Oh, "Monolithically Integrated Multiwavelength Grating Cavity Laser," *IEEE Photon. Tech. Lett*., vol. 17, Sep. 2005, pp. 1788-1790.

[30] J. H. Ahn, K. R. Oh, J. S. Kim, S. W. Lee, H. M. Kim, K. E. Pyun, and H. M. Park, "Uniform and High Coupling Efficiency Between InGaAsP-InP Buried Heterostructure Optical Amplifier and Monolithically Butt-Coupled Waveguide Using Reactive Ion Etching," *IEEE Photon. Technol. Lett.*, vol. 8, no. 2, Feb. 1996, pp. 200-202.

[31] A. P. A Fischer, M. Yousefi, D. Lenstra, M. W. Carter, and G. Vemuri, "Experimental and Theoretical Study of Semiconductor Laser Dynamics Due to Filtered Optical Feedback," *IEEE J. Select. Topics Quantum Electron*., vol. 10, no. 5, Sep.-Oct. 2004, pp. 944-954.

[32] K. H. Kim, O. K. Kwon, J. H. Kim, E. D. Sim, H. S. Kim, and K. R. Oh, "Monolithically Integrated External Cavity Wavelength Tunable Laser Using Beam Steering Controller," *IEE Electron. Lett*., vol. 41, no. 21, Oct. 2005, pp. 1173-1175.

[33] A. A. Tager, "Side-Mode Suppression for Long DBR Lasers," *IEEE Photon. Technol. Lett.*, vol. 7, no. 8, Aug. 1995, pp. 866-868.

[34] C. R. Doerr, M. Zirngibl, and C. H. Joyner, "Single Longitudinal-Mode Stability Via Wave Mixing in Long-Cavity Semiconductor Lasers," *IEEE Photon. Technol. Lett.*, vol. 7, no. 9, Sep. 1995, pp. 962-964.

[35] C. R. Doerr, "Theoretical Stability Analysis of Side-Mode Operation in Uncontrolled Mode-Selection Semiconductor Lasers," *IEEE Photon. Technol. Lett.*, vol. 9, no. 11, Nov. 1997, pp. 1457-1459.

[36] A. P. Bogatov, P. G. Eliseev, and B. N. Sverdlov, "Anomalous Interaction of Spectral Modes in a Semiconductor Laser," *IEEE J. Quantum Electron.*, vol. QE-11, no. 7, July 1975, pp. 510-515.

[37] A. Godard, G. Pauliat, G. Roosen, and E. Ducloux, "Modal Competition Via Four-Wave Mixing in Single-Mode Extended-Cavity Semiconductor Lasers," *IEEE J. Quantum Electron*., vol. 40, Aug. 2004, pp. 970-981.

[38] O. K. Kwon, K. H. Kim, E. D. Sim, J. H. Kim, H. S. Kim, and K. R. Oh, "Broadly Wavelength-Tunable External Cavity Lasers with Extremely Low Power Variation over Tuning Range," *IEEE Photon. Technol. Lett.*, vol. 17, no. 3, Mar. 2005, pp. 537-539.

[39] C. Thirstrup, "Refractive Index Modulation Based on Excitonic Effects in GaInAs-InP Coupled Asymmetric Quantum Wells," *IEEE J. Quantum Electron.*, vol. 31, no. 6, June 1993, pp. 988-996.

Oh-Kee Kwon received the BS and MS degrees in electronic engineering from Hanyang University, Korea, in 1996 and 1998, respectively. From 1998 to 2002, he served in Logistics Command, Korea Air Force as an officer. In 2002, he joined the Basic Research Laboratory (currently ICCL) of ETRI where he is engaged in work on broad gain lasers, multi-wavelength lasers, and tunable lasers for WDM application. He received the Excellent Paper Award in 2006 from COOC in 2005. His name was included in 9th edition of *Marquis Who's Who in Science and Engineering* (Sept. 2006) for distinguished results in the fields of semiconductor lasers.

Eundeok Sim received the BS, MS, and PhD degrees in physics from Yonsei University, Korea, in 1994, 1996, and 2001, respectively. He joined the Basic Research Laboratory of Electronics and Telecommunication Research Institute (ETRI) in 2001 and has worked on InP-based optoelectronic devices.

Kang-Ho Kim received the BS and MS degrees in physics from Dong-Ah University, Korea, in 1994 and 1996 and the PhD degree in physics from Ulsan University in 2004. He joined ETRI in 2001. From 2001 to 2005, he was involved in work on WDM devices based on semiconductor lasers, such as wavelength tunable lasers. He is currently working in LED/SSL R&DB Sector of Korea Photonics Technology Institute.

Jong-Hoi Kim received the BS, MS, and PhD degrees in physics from Sogang University, Korea, in 1993, 1995, and 2000, respectively. In 2000, he joined the Basic Research Laboratory of Electronics and Telecommunication Research Institute (ETRI) where he is engaged in work on all-optical functional devices based on semiconductor optical amplifiers, such as all-optical wavelength converters and all-optical gate switches.

Ho-Gyeong Yun received the BS degree in 1998 followed by the MS degree in 2000, both in materials science and engineering from Korea University, Korea. In 2000, he developed PDP using LTCC-M process for LG Electronics. He has been a Senior Research Engineer at ETRI since 2005, where he has been designing high-speed modules over 40 GHz with electrical simulation and measurement. Currently, his research area includes the development of 40G modules for optical telecommunication application.

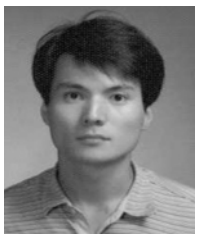

O Kyun Kwon received MS and PhD degrees in material science and engineering from KAIST, Korea. In 1991, he joined the Basic Research Laboratory of Electronics and Telecommunication Research Institute (ETRI) where he is engaged in work on all-optical logic devices, optical interconnection devices, and vertical cavity surface emitting lasers.

Kwang Ryong Oh joined the Electronics and Telecommunication Research Institute (ETRI), Korea, as a Researcher in 1985, where he was involved in the characterization and development of long wavelength semiconductor lasers and PIN + JFET OEIC. Since 1992, he has been involved in the area of the optical switches, such as TIR and LD gate optical switches. His current research areas are WDM optical devices, such as SOAs, wavelength converters, and tunable laser diodes.